2806 *Inorg. Chem.* **1986**, *25*, 2806–2812

Contribution from the Department of Chemistry,
Colorado State University, Fort Collins, Colorado 80523

An Unusual Hydrogen Bond between Oxygen Atoms: Preparation and Characterization of $[N(n\text{-Bu})_4^+][H(OTeF_5)_2^-]$

Steven H. Strauss,* Kent D. Abney, and Oren P. Anderson

Received January 8, 1986

The compound $[N(n\text{-Bu})_4^+][H(OTeF_5)_2^-]$ was prepared from $HOTeF_5$ and $[N(n\text{-Bu})_4^+][OTeF_5^-]$. It crystallizes in the triclinic system, space group $P\bar{1}$ (No. 2). Unit cell parameters are $a = 9.838$ (3) Å, $b = 9.938$ (3) Å, $c = 14.324$ (4) Å, $\alpha = 71.89$ (2)°, $\beta = 83.31$ (2)°, $\gamma = 79.72$ (2)°, and $Z = 2$. The $H(OTeF_5)_2^-$ ion is unusual in several respects. NMR and IR spectral data suggest that it contains a very strong O–H–O hydrogen bond. Unlike all other discrete HA_2^- ions (A^- = the anion of a hydroxy-containing acid), which have O···O distances <2.5 Å, the O···O distance in $H(OTeF_5)_2^-$ is 2.595 (8) Å (2.564 Å with librational correction). Therefore, despite the fluorine-like behavior of the $OTeF_5$ moiety, the O–H–O hydrogen bond in the $H(OTeF_5)_2^-$ anion does not rival bifluoride ion (HF_2^-) as the strongest, shortest hydrogen bond. Furthermore, while there is no precedent for an O–H–O hydrogen bond to have an O–H distance >1.1 Å and an O···O distance >2.5 Å, such a situation in $H(OTeF_5)_2^-$ is supported by structural, NMR, IR, and Raman data.

Introduction

A great many main-group and high-valent transition-metal compounds of the pseudohalogen $OTeF_5$ have been studied[1–3] since the discovery of $HOTeF_5$ in 1964.[4] There is a wealth of physicochemical data that points to an electronic similarity between $OTeF_5$ and fluorine.[1–3,5] One impressive fact is that this bulky and electronegative substituent forms stable compounds such as $I(OTeF_5)_5$,[6] $Xe(OTeF_5)_6$,[7] and $U(OTeF_5)_6$[8] that have few (if any) analogues outside of the corresponding fluorides. The bonding between the central atom and oxygen in many of these compounds is undoubtedly largely covalent. We have been exploring the use of $OTeF_5^-$ (hereafter referred to as teflate[9]) as a ligand in low-valent transition-metal complexes. In compounds such as $Mn(OTeF_5)(CO)_5$,[10] $[AgOTeF_5(C_6H_5CH_3)_2]_2$,[11] $Pt(OTeF_5)_2(\text{diene})$,[12] and $Fe(OTeF_5)_3$,[13] the teflate groups have considerable ionic character. We wondered whether the electronic analogy between $OTeF_5$ and fluorine for main-group compounds could be extrapolated to a parallel analogy between teflate and fluoride for transition-metal chemistry. One potential way to probe for pseudo-fluoride behavior is to examine the propensity of a species to form very strong hydrogen bonds, similar to that in bifluoride ion (HF_2^-), which contains the strongest known hydrogen bond.[14–19] To this end, we have prepared the compound $[N(n\text{-Bu})_4^+][H(OTeF_5)_2^-]$ and have characterized it by X-ray crystallography and by NMR and vibrational spectroscopy, and herein we report our findings.

Experimental Section

General Procedures. In the following preparations and physical measurements, all operations were carried out with rigorous exclusion of dioxygen and water. Schlenk, glovebox, and high-vacuum techniques were employed, with purified dinitrogen used when an inert atmosphere was required.

Reagents and Solvents. The following solvents were dried by distillation from the indicated drying agent: hexane (Na), dichloromethane (CaH_2), dichloromethane-d_2 (CaH_2), ethyl acetate (P_2O_5), chloroform-d (4-Å molecular sieves), acetonitrile-d_3 (4-Å sieves), triethylamine (BaO). Fluorosulfonic acid (HSO_3F, Fluka) was used as received unless otherwise specified. Telluric acid ($Te(OH)_6$, Cerac) and sulfuric acid-d_2 (D_2SO_4, 99% D, Stohler) were used as received. Water was removed from an ethyl acetate solution of $N(n\text{-Bu})_4Cl$ (Aldrich) by azeotropic distillation. The anhydrous, crystalline salt was dried under vacuum at room temperature to remove any traces of ethyl acetate.

Physical Measurements. Samples for NMR spectroscopy were dichloromethane, dichloromethane-d_2, chloroform-d, or acetonitrile-d_3 solutions with 1% $CFCl_3$ and/or 1% Me_4Si added. Chemical shifts (δ scale) are relative to these internal standards for ^{19}F and ^1H NMR spectra. All spectra were recorded on a Bruker SY-200 spectrometer at the indicated frequencies: ^{19}F, 188.31 MHz; ^1H, 200.13 MHz. All ^{19}F NMR spectra were AB_4X patterns upfield of $CFCl_3$, unless otherwise noted ($X = {}^{125}Te$, 7.0% NA, $I = {}^1/_2$).

Samples for IR spectroscopy were mulls (Nujol or Fluorolube, KBr windows) or dichloromethane solutions (0.2-mm path length Irtran-2 cells). Spectra were recorded on a Perkin-Elmer 983 spectrometer calibrated with polystyrene. Band positions are ±1 cm^{-1}. Samples for Raman spectroscopy were crystalline or polycrystalline solids loaded into glass capillaries. Spectra were recorded with a Spex Ramalog 5 spectrometer calibrated with standard compounds. The 514.5-nm line of an argon ion laser was used.

Preparation of Compounds. $HOTeF_5$. The compound was prepared by modification of literature procedures.[20,21] Telluric acid (50 g, 0.22 mol) and fluorosulfonic acid (150 mL, 260 g, 2.6 mol) were carefully mixed at −78 °C in a 500-mL round-bottom flask. Water (1 mL) was carefully added dropwise to the cold reaction mixture, which was then refluxed under nitrogen through a Vigreaux column attached to a −78 °C cold finger positioned over a 100-mL Schlenk flask, which was also cooled to −78 °C. As the product $HOTeF_5$ distilled out of the reaction mixture, the temperature at the top of the Vigreaux column rose from 50 to 110 °C during the course of 2 h. The crude product condensed on the cold finger as crystalline white flakes, which fell off and were collected in the Schlenk flask. The crude product (75–85% based on $Te(OH)_6$) contained small amounts of HF and HSO_3F and varying amounts of $Te_2O_2F_8$.[22] The latter compound was identified by its ^{19}F NMR spectrum (CH_2Cl_2, A_2B_2X pattern, δ_A −50.0, δ_B −22.3, J_{AB} = 193

---

(1) Seppelt, K. *Angew. Chem., Int. Ed. Engl.* **1982**, *21*, 877.
(2) Engelbrecht, A.; Sladky, F. *Adv. Inorg. Chem. Radiochem.* **1981**, *24*, 189.
(3) Seppelt, K. *Acc. Chem. Res.* **1979**, *12*, 211.
(4) Engelbrecht, A.; Sladky, F. *Angew. Chem., Int. Ed. Engl.* **1964**, *3*, 383.
(5) Birchall, T.; Myers, R. D.; DeWaard, H.; Schrobilogen, G. J. *Inorg. Chem.* **1982**, *21*, 1068.
(6) Seppelt, K.; Lentz, D. *Z. Anorg. Allg. Chem.* **1980**, *460*, 5.
(7) Lentz, D.; Seppelt, K. *Angew. Chem., Int. Ed. Engl.* **1979**, *18*, 66.
(8) (a) Seppelt, K. *Chem. Ber.* **1976**, *109*, 1046. (b) Templeton, L. K.; Templeton, D. H.; Bartlett, N.; Seppelt, K. *Inorg. Chem.* **1976**, *15*, 2720.
(9) We suggest the abbreviations teflate and teflic acid in place of the correct nomenclature pentafluoroorthotellurate and pentafluoroorthotelluric acid, respectively. The latter compound is the parent from which all teflates are prepared.[1–3]
(10) Strauss, S. H.; Abney, K. D.; Long, K. M.; Anderson, O. P. *Inorg. Chem.* **1984**, *23*, 1994.
(11) Strauss, S. H.; Noirot, M. D.; Anderson, O. P. *Inorg. Chem.* **1985**, *24*, 4307.
(12) Strauss, S. H.; Colsman, M. R.; Manning, M. C., manuscript in preparation.
(13) Strauss, S. H.; Miller, P. K., manuscript in preparation.
(14) Hamilton, W. C.; Ibers, J. A. *Hydrogen Bonding in Solids*; Benjamin: San Francisco, 1968.
(15) Joesten, M. D.; Schaad, L. J. *Hydrogen Bonding*; Marcel Dekker: New York, 1974.
(16) Novak, A. *Struct. Bonding (Berlin)* **1974**, *18*, 177.
(17) Schuster, P., Zundel, G., Sandorfy, C., Eds. *The Hydrogen Bond*; North-Holland: Amsterdam, 1976; Vols. 1–3.
(18) Emsley, J. *Chem. Soc. Rev.* **1980**, *9*, 91.
(19) Hadzi, D. *J. Mol. Struct.* **1983**, *100*, 393.
(20) Seppelt, K.; Nothe, D. *Inorg. Chem.* **1973**, *12*, 2727.
(21) Schack, C. J.; Wilson, W. W.; Christe, K. O. *Inorg. Chem.* **1983**, *22*, 18.
(22) Seppelt, K. *Angew. Chem., Int. Ed. Engl.* **1974**, *13*, 92.

0020-1669/86/1325-2806$01.50/0

Hz; lit.,[22] neat $CFCl_3$, δ_A −53.5, δ_B −25.6, J_{AB} = 189 Hz). The amount of this compound present in the crude product (as much as 5% in some preparations) can be minimized (~0%) by ensuring that a sufficient amount of HF (i.e. added H_2O) is present in the reaction mixture. If $HOTeF_5$ is prepared on a regular basis, the round-bottom flask, Vigreaux column, and thermometer have to be replaced every few preparations.

The crude product was vacuum-distilled through −42, −78, and −196 °C cold traps. The −42 and −196 °C traps retained HSO_3F and HF, respectively. The −78 °C trap contained $HOTeF_5$ and any $Te_2O_2F_8$. These two compounds cannot be separated by vacuum distillation through cold traps. The final purification was achieved by adding a small amount of $[N(n\text{-}Bu)_4^+][OTeF_5^-]$ (see below) and heating the mixture to 60 °C for several days. At this point, pure $HOTeF_5$ (mp 40 °C, bp 60 °C[4]) was vacuum-transferred out of the mixture.[23] The overall purified yield was 70–80% based on $Te(OH)_6$. ^{19}F NMR (CH_2Cl_2): δ_A −42.4, δ_B −45.8, J_{AB} = 174 Hz, J_{AX} = 3490 Hz, J_{BX} = 3602 Hz.

$[N(n\text{-}Bu)_4^+][OTeF_5^-]$. A solution of $N(n\text{-}Bu)_4Cl$ (7.89 g, 28.4 mol) in dichloromethane (40 mL) was added dropwise to a −30 °C solution of $HOTeF_5$ (6.82 g, 28.4 mol) in dichloromethane (30 mL). Hydrogen chloride was vented through a −78 °C trap to a mineral oil bubbler. Once the addition was complete, the mixture was warmed to room temperature and all volatiles were removed under vacuum, leaving a fluffy white powder. Recrystallization from ethyl acetate/hexane afforded large colorless crystals in 85% yield. ^{19}F NMR (CH_2Cl_2): δ_A −19.0, δ_B −36.8, J_{AB} = 148 Hz, J_{AX} = 2664 Hz, J_{BX} = 3654 Hz.

$DOTeF_5$. All reaction tubes and the vacuum line used for this preparation were pretreated with D_2O for 24 h and then flamed out under vacuum. Solid $[N(n\text{-}Bu)_4^+][OTeF_5^-]$ was treated with a >10-fold excess of sulfuric acid-d_2. The mixture was vacuum-distilled through −42 and −78 °C traps. The −78 °C trap contained $DOTeF_5$ in >95% yield. The % D in the product can be estimated from the intensities of the $\nu(OD)$ (2670 cm^{-1}) and $\nu(OH)$ (3618 cm^{-1}, $HOTeF_5$[24]) bands in the gas-phase IR spectrum (Irtran-2 windows) of the product. If care is taken to pretreat all glassware as described above, the % D can exceed 95%. The ^{19}F NMR spectrum of this compound in dichloromethane is identical with that of $HOTeF_5$.

$[N(n\text{-}Bu)_4^+][H(OTeF_5)_2^-]$. Stoichiometric amounts of $HOTeF_5$ and $[N(n\text{-}Bu)_4^+][OTeF_5^-]$ were mixed in dichloromethane. Slow evaporation of a hexane/dichloromethane solution resulted in the formation of large, colorless crystals in 80% yield. ^{19}F NMR (CH_2Cl_2): δ_A −32.1, δ_B −44.8, J_{AB} = 172 Hz, J_{AX} = 3066 Hz, J_{BX} = 3552 Hz. The compound $[N(n\text{-}Bu)_4^+][D(OTeF_5)_2^-]$ was prepared with $DOTeF_5$ in place of $HOTeF_5$. The ^{19}F NMR spectrum of this compound in dichloromethane is identical with that of $[N(n\text{-}Bu)_4^+][H(OTeF_5)_2^-]$.

$[N(n\text{-}Bu)_4^+][SO_3F^-]$. A solution of freshly distilled fluorosulfonic acid (0.069 g, 0.040 mL, 0.69 mmol) in dichloromethane (5 mL) was added dropwise to a stirred solution of $N(n\text{-}Bu)_4Cl$ (0.19 g, 0.69 mmol) in dichloromethane (5 mL). Hydrogen chloride was vented through a mineral oil bubbler. All volatiles were removed under vacuum, leaving a white powder that was used without further purification.

$[N(n\text{-}Bu)_4^+][H(SO_3F)_2^-]$. Stoichiometric amounts of freshly distilled fluorosulfonic acid and $[N(n\text{-}Bu)_4^+][SO_3F^-]$ were mixed in dichloromethane. All volatiles were removed under vacuum, leaving a white powder that was used without further purification. ^1H NMR ($CDCl_3$): δ 15.40.

$[NEt_3H^+][OTeF_5^-]$. Stoichiometric amounts of triethylamine and $HOTeF_5$ were mixed in dichloromethane. Slow addition of pentane by vapor diffusion affords large, colorless crystals in >80% yield. ^{19}F NMR (CH_2Cl_2): δ_A −25.4, δ_B −40.4, J_{AB} = 174 Hz, J_{AX} = 2856 Hz, J_{BX} = 3588 Hz. ^1H NMR (CH_2Cl_2): δ 10.32.

Crystallographic Study. A colorless platelet of $[N(n\text{-}Bu)_4^+][H(OTeF_5)_2^-]$ was centered on a Nicolet R3m diffractometer. Centering of 25 reflections allowed least-squares calculation[25] of the cell constants given in Table I. The unit cell parameters were submitted to the cell reduction program TRACER (obtained from J. A. Ibers); no cell of higher symmetry was found. Relevant experimental parameters and results are listed in Table I.

Since several crystals showed considerable deterioration upon long exposure to the X-ray beam using standard θ–2θ scans, the intensities of all reflections were measured with Wyckoff ω scans with seven step counts. The intensities of control reflections (210, 014, 041) monitored every 97 reflections showed no significant trend during the course of the data collection. The data were collected at −130 °C after it was found that the structure was disordered at room temperature. The crystal was cooled slowly, after several crystals cracked upon sudden cooling. ω plots were performed to check the crystal for cracking or twinning.

Table I. Details of the X-ray Diffraction Study

mol formula	$[N(n\text{-}Bu)_4^+][H(OTeF_5)_2^-]$, $C_{16}H_{37}F_{10}NO_2Te_2$
mol wt	720.66
space group	$P\bar{1}$
unit cell	
a, Å	9.838(3)
b, Å	9.938(3)
c, Å	14.324(4)
α, deg	71.89(2)
β, deg	83.31(2)
γ, deg	79.72(2)
unit cell vol, Å^3	1306.8
Z	2
calcd density, g cm^{-3}	1.83
cryst dimens, mm^3	0.36 × 0.12 × 0.38
data collcn temp,[a] °C	−130
radiation (λ, Å)	Mo Kα (0.71073)
monochromator	graphite
abs coeff, cm^{-1}	23.88
2θ range, deg	3.5–50
reflcns:	$h \geq 0$, $\pm k$, $\pm l$
no. of reflcns with $I > 2\sigma(I)$	3819
total no. of reflcns measd	5048
scan type	ω, Wyckoff
scan speed, deg min^{-1}	5–30, variable
data/param ratio	13.1
R	0.038
R_w	0.042
GOF	1.713
g (refined)	3.6 × 10^{-4}
slope of normal probability plot	1.53

[a] Obtained with a Nicolet LT-1 accessory.

An empirical absorption correction was applied to the observed data, based on intensity profiles for 11 reflections over a range of setting angles (ψ) for the diffraction vector. Transmission factors ranged from 0.868 to 0.551. Lorentz and polarization corrections were applied to the data.

The tellurium atoms were located by Patterson methods, and all other non-hydrogen atoms were located in subsequent difference Fourier maps. The refinement involved anisotropic thermal parameters for all non-hydrogen atoms. Neutral-atom scattering factors (including anomalous scattering) were taken from ref 26. The hydrogen atom that bridges the two oxygen atoms was not located. Other hydrogen atoms were included in calculated positions 0.96 Å from carbon atoms, with isotropic thermal parameters 20% higher than the equivalent isotropic thermal parameter for the carbon atom to which they were attached. The weighted least-squares refinement (weights calculated as $(\sigma^2(F) + g^2F_o^2)^{-1}$) converged, with the average shift/esd = 0.012 over the last eight cycles.

In the final difference Fourier synthesis, the maximum electron density was 0.97 e Å^{-3} in the immediate vicinity of a fluorine atom. The minimum electron density was −0.54 e Å^{-3}. Analysis of variance as a function of Bragg angle, magnitude of F_o, reflection indices, etc. showed no significant trends.

Tables II and III contain a list of atomic positional parameters and equivalent isotropic thermal parameters and a list of interatomic distances and angles, respectively, for $[N(n\text{-}Bu)_4^+][H(OTeF_5)_2^-]$. Available as supplementary material are lists of anisotropic thermal parameters for all non-hydrogen atoms (Table S-I), hydrogen atom positions and isotropic thermal parameters (Table S-II), and observed and calculated structure factors (Table S-III). See paragraph at end of paper regarding supplementary material.

Results

Structure of $[N(n\text{-}Bu)_4^+][H(OTeF_5)_2^-]$. This salt crystallized in the triclinic system, space group $P\bar{1}$. The packing consists of two symmetry-related formula units per unit cell. Figure S-1 (supplementary material[27]) is a drawing of the $N(n\text{-}Bu)_4^+$ cation

---

(23) Presumably, $OTeF_5^-$ reacts with $Te_2O_2F_8$ to form a nonvolatile polymer, $F_5TeO(TeOF_4)_n^-$: Abney, K. D.; Strauss, S. H., unpublished data, 1985.

(24) Burger, H. *Z. Anorg. Allg. Chem.* **1968**, *360*, 97.

(25) Calculations for diffractometer operations were performed by using software supplied with the Nicolet R3m diffractometer. All structural calculations were performed on the Data General Eclipse S/140 computer in the X-ray laboratory at Colorado State University with the SHELXTL program library written by Professor G. M. Sheldrick and supplied by Nicolet XRD Corp.

(26) *International Tables for X-ray Crystallography*; Kynoch: Birmingham, England, 1974; Vol. IV.

Table II. Atomic Coordinates ($\times 10^4$) and Isotropic Thermal Parameters ($Å^2 \times 10^3$)[a] for $[N(n\text{-}Bu)_4^+][H(OTeF_5)_2^-]$

atom	x	y	z	U_{iso}[b]
Te1	2760 (1)	2263 (1)	446 (1)	33 (1)
O1	1478 (4)	1653 (5)	1417 (3)	60 (2)
F1	1481 (5)	3673 (5)	−244 (4)	127 (3)
F2	4181 (4)	941 (5)	969 (5)	115 (3)
F3	3960 (6)	2932 (6)	−588 (4)	113 (3)
F4	2356 (7)	1074 (6)	−195 (4)	116 (3)
F5	3268 (6)	3559 (5)	920 (4)	113 (3)
Te2	2516 (1)	9421 (1)	3875 (1)	34 (1)
O2	2292 (7)	11278 (5)	3152 (4)	83 (2)
F6	4207 (4)	9539 (5)	4231 (3)	85 (2)
F7	837 (4)	9128 (6)	3661 (4)	86 (2)
F8	2778 (5)	7587 (4)	4667 (3)	87 (2)
F9	3320 (4)	8729 (4)	2878 (3)	69 (2)
F10	1746 (4)	9889 (4)	4976 (3)	70 (2)
N1	2658 (4)	−2343 (4)	7949 (3)	21 (1)
C1	2043 (4)	−792 (4)	7476 (3)	20 (1)
C2	2903 (5)	321 (4)	7509 (4)	27 (2)
C3	2340 (5)	1788 (5)	6845 (4)	28 (2)
C4	3150 (5)	2931 (5)	6860 (4)	36 (2)
C5	2998 (5)	−2584 (5)	9003 (3)	25 (2)
C6	1795 (5)	−2167 (5)	9676 (3)	26 (2)
C7	2255 (6)	−2517 (6)	10723 (4)	37 (2)
C8	1085 (6)	−2091 (6)	11414 (4)	41 (2)
C9	4000 (4)	−2687 (4)	7355 (3)	21 (1)
C10	4641 (5)	−4254 (5)	7619 (4)	28 (2)
C11	5994 (5)	−4462 (5)	7003 (4)	32 (2)
C12	5835 (6)	−4080 (7)	5917 (4)	44 (2)
C13	1620 (4)	−3306 (4)	7960 (3)	21 (1)
C14	1217 (5)	−3269 (5)	6957 (3)	24 (2)
C15	205 (5)	−4313 (5)	7091 (4)	29 (2)
C16	−219 (6)	−4353 (6)	6112 (4)	41 (2)

[a] Estimated standard deviations in the least significant digits are given in parentheses. [b] Equivalent isotropic U defined as one-third of the trace of the orthogonalized U_{ij} tensor.

Table III. Bond Lengths (Å)[a] and Bond Angles (deg)[a] for $[N(n\text{-}Bu)_4^+][H(OTeF_5)_2^-]$

Te1–O1	1.798 (4)	Te1–F1	1.823 (5)
Te1–F2	1.793 (4)	Te1–F3	1.815 (5)
Te1–F4	1.823 (7)	Te1–F5	1.795 (7)
Te2–O2	1.802 (4)	Te2–F6	1.829 (5)
Te2–F7	1.803 (5)	Te2–F8	1.814 (4)
Te2–F9	1.814 (4)	Te2–F10	1.825 (4)
N1–C1	1.521 (5)	N1–C5	1.521 (6)
N1–C9	1.529 (5)	N1–C13	1.515 (6)
C1–C2	1.522 (7)	C2–C3	1.520 (6)
C3–C4	1.506 (8)	C5–C6	1.519 (6)
C6–C7	1.533 (7)	C7–C8	1.518 (8)
C9–C10	1.518 (6)	C10–C11	1.528 (7)
C11–C12	1.501 (8)	C13–C14	1.522 (7)
C14–C15	1.518 (7)	C15–C16	1.522 (9)
O1–Te1–F1	91.4 (2)	O1–Te1–F2	96.7 (2)
F1–Te1–F2	171.8 (2)	O1–Te1–F3	176.1 (2)
F1–Te1–F3	85.0 (2)	F2–Te1–F3	86.9 (2)
O1–Te1–F4	90.3 (2)	F1–Te1–F4	88.9 (3)
F2–Te1–F4	89.6 (3)	F3–Te1–F4	88.2 (3)
O1–Te1–F5	97.1 (3)	F1–Te1–F5	88.5 (3)
F2–Te1–F5	91.9 (3)	F3–Te1–F5	84.3 (3)
F4–Te1–F5	172.2 (2)	O2–Te2–F6	91.6 (3)
O2–Te2–F7	94.6 (3)	F6–Te2–F7	173.0 (2)
O2–Te2–F8	176.2 (3)	F6–Te2–F8	85.7 (2)
F7–Te2–F8	87.9 (2)	O2–Te2–F9	95.9 (2)
F6–Te2–F9	91.3 (2)	F7–Te2–F9	91.2 (2)
F8–Te2–F9	87.0 (2)	O2–Te2–F10	91.2 (2)
F6–Te2–F10	88.0 (2)	F7–Te2–F10	88.8 (2)
F8–Te2–F10	86.0 (2)	F9–Te2–F10	172.9 (2)
C1–N1–C5	111.1 (4)	C1–N1–C9	108.3 (3)
C5–N1–C9	108.4 (3)	C1–N1–C13	109.2 (3)
C5–N1–C13	108.5 (3)	C9–N1–C13	111.4 (4)
N1–C1–C2	115.4 (4)	C1–C2–C3	110.5 (4)
C2–C3–C4	112.4 (4)	N1–C5–C6	115.4 (4)
C5–C6–C7	110.3 (4)	C6–C7–C8	111.8 (4)
N1–C9–C10	115.6 (3)	C9–C10–C11	111.0 (4)
C10–C11–C12	114.5 (4)	N1–C13–C14	115.9 (3)
C13–C14–C15	109.5 (4)	C14–C15–C16	112.3 (4)

[a] Estimated standard deviations in the least significant digits are given in parentheses.

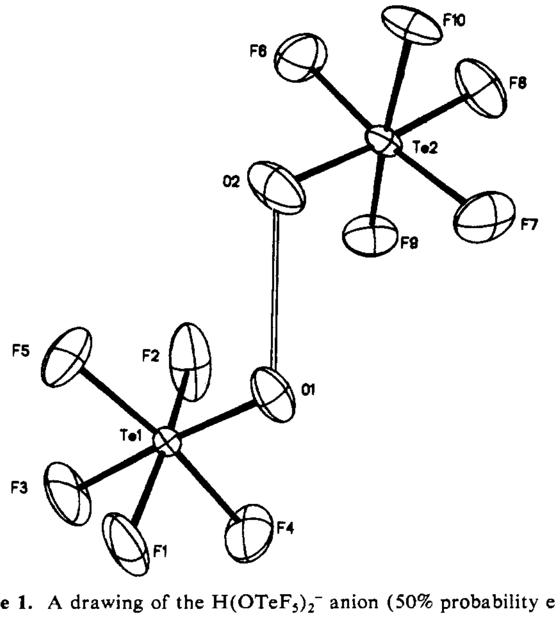

Figure 1. A drawing of the $H(OTeF_5)_2^-$ anion (50% probability ellipsoids).

showing the numbering scheme used. There are no unusually short contacts between cations, between anions, or between the cations and the anions. A stereoview of the packing of the salt in the unit cell is shown in Figure S-2.[27] Bond distances and angles within the $N(n\text{-}Bu)_4^+$ cation are normal.

A drawing of the $H(OTeF_5)_2^-$ anion is shown in Figure 1. Interatomic distances and angles for the anion are collected in Table III. Since the O1···O2 distance of 2.595 (8) Å is considerably shorter than twice the van der Waals radius for oxygen (2.80 Å[28]), there is little doubt that the proton, which was not located, lies somewhere between the oxygen atoms of the two octahedral teflate anions, although it does not have to lie directly on the O1–O2 vector. Note that the two oxygen and two tellurium atoms are not coplanar: the dihedral angle between the Te1–O1–O2 and Te2–O2–O1 planes is 113°.

The $H(OTeF_5)_2^-$ anion, which does not possess any crystallographically imposed symmetry, has approximate C_2 symmetry with the pseudo-C_2 axis bisecting the O1–O2 vector; the two tellurium–oxygen distances are equal to within one standard deviation, and the Te1–O1–O2 and Te2–O2–O1 angles, 112.8 and 112.3°, respectively, are virtually identical. However, the asymmetry of the anion is seen by comparing the distances from the center of the O1–O2 vector (Ct) to the four closest fluorine atoms: Ct···F2 = 2.850 Å, Ct···F5 = 2.804 Å, Ct···F7 = 2.807 Å, Ct···F9 = 2.754 Å. This asymmetry is paralleled by the closest fluorine–oxygen distances between teflate groups in the $H(OTeF_5)_2^-$ anion: F2···O2 = 3.524 (8) Å, F5···O2 = 3.440 (7) Å, F9···O1 = 3.366 (5) Å, F7···O1 = 3.479 (6) Å. The closest fluorine–fluorine distance between teflate groups in the $H(OTeF_5)_2^-$ anion is 3.069 (6) Å for F2···F9; other distances of this type were all greater than 4.4 Å.

The oxygen and fluorine atoms of the two $OTeF_5$ moieties exhibit large amplitude thermal motion (see Tables II and S-I), despite the low temperature at which the data set was collected. Examination of the thermal ellipsoids (see Figure 1) suggested that these two groups might be executing rigid-body librational motion, and a standard analysis of this type was performed.[29]

---

(27) See paragraph at end of text regarding supplementary material.

(28) Pauling, L. *The Nature of the Chemical Bond*, 3rd ed.; Cornell University Press: Ithaca, NY, 1960; p 260.

Table IV. Librational Corrections to Te–X Bond Lengths

bond	cor, Å	cor length, Å	bond	cor, Å	cor length, Å
Te1–O1	0.043	1.841	Te2–O2	0.041	1.843
Te1–F1	0.063	1.886	Te2–F6	0.041	1.870
Te1–F2	0.064	1.857	Te2–F7	0.041	1.843
Te1–F3	0.044	1.859	Te2–F8	0.041	1.855
Te1–F4	0.070	1.894	Te2–F9	0.028	1.842
Te1–F5	0.063	1.858	Te2–F10	0.028	1.853

Table V. ^1H NMR Data[a]

solvent	compd or ion	counterion	concn, M	δ^b
$CDCl_3$	$HOTeF_5$		0.060	5.70
			2.6	5.65
	HSO_3F		0.050	7.76
	$H(OTeF_5)_2^-$	$N(n\text{-}Bu)_4^+$	0.150	16.24
	$H(SO_3F)_2^-$	$N(n\text{-}Bu)_4^+$	0.200	15.40
	$H(CH_3CO_2)_2^-$	$N(n\text{-}Bu)_4^+$	*c*	15.7[c]
	$H(CF_3CO_2)_2^-$	$N(n\text{-}Bu)_4^+$	*c*	18.2[c]
CD_2Cl_2	$HOTeF_5$		0.050	6.37
	$H(OTeF_5)_2^-$	$N(n\text{-}Bu)_4^+$	0.050	16.42
CD_3CN	$HOTeF_5$		0.050	10.15
			1.9	10.75
	$H(OTeF_5)_2^-$	$N(n\text{-}Bu)_4^+$	0.700	16.57
	$H(NO_3)_2^-$	$As(C_6H_5)_4^+$	0.080	14.81[d]
	HF_2^-	NEt_4^+	0.050	16.29[e]

[a] All data from this work, unless otherwise noted. [b] ^1H chemical shift, $Me_4Si = 0$. [c] Extrapolated to infinite dilution.[30a] [d] Reference 30b. [e] Reference 31.

That analysis was highly successful ($R = 0.087$ for the $OTeF_5$ group containing Te1 and $R = 0.067$ for the Te2 group). As expected, this analysis resulted in longer Te–O and Te–F bonds; with the librational correction, Te1–O1 was longer by 0.043 Å, at 1.841 Å, while Te2–O2 was longer by 0.041 Å, at 1.843 Å. Due to the offset orientation of these two Te–O bonds, the O1···O2 hydrogen bond distance was only shortened by 0.031 Å, to 2.564 Å. The librational correction resulted in Te–F bonds longer by 0.028–0.070 Å (see Table IV).

NMR Spectroscopy. Proton NMR data are collected in Table V, which also contains relevant data from the literature for comparison.[29-31] The ^1H chemical shift for the strong acid[32] $HOTeF_5$, δ 5.70 in $CDCl_3$ and δ 6.37 in CD_2Cl_2, is in accord with the literature value of δ 5.58 in $CFCl_3$.[33] A large downfield shift to δ 10.15 is observed in the more basic solvent CD_3CN, presumably due to hydrogen bonding between teflic acid[9] and solvent. Even larger downfield shifts ($\delta > 15$) are observed for the proton in bifluoride ion and for protons bridging two oxo anions including teflate, acetate, trifluoroacetate, fluorosulfate, and nitrate. Note that the ^1H NMR chemical shift for $H(OTeF_5)_2^-$ is not very solvent-dependent.

Fluorine-19 NMR data (chemical shifts and coupling constants) are found in the Experimental Section for each individual compound. The AB_4X pattern, typical of teflates,[33,34] is always upfield of δ for $CFCl_3$. Figure 2 shows the large downfield shift experienced by δ_A as the ionic character of the teflate group increases.

Vibrational Spectroscopy. Table VI contains IR and Raman data for $HOTeF_5$, $DOTeF_5$, $[N(n\text{-}Bu)_4^+][OTeF_5^-]$, $[NEt_3H^+][OTeF_5^-]$, $[N(n\text{-}Bu)_4^+][H(OTeF_5)_2^-]$, and $[N(n\text{-}Bu)_4^+][D(OTeF_5)_2^-]$. The gas-phase IR data for $HOTeF_5$ agree well with those of an earlier report.[24] The bands attributable to ν(OH) and ν(OD) in the gas phase, 3618 and 2670 cm^{-1}, respectively (3618/2670 = 1.35), are shifted to lower energy in dichloromethane solution: 3424 and 2536 cm^{-1}, respectively, for $HOTeF_5$ and $DOTeF_5$ (3424/2536 = 1.35). These bands completely disappear upon addition of exactly 1 equiv of $[N(n\text{-}Bu)_4^+][OTeF_5^-]$. In the case of $HOTeF_5$, addition of $OTeF_5^-$ results in a new very broad band centered at 1150 cm^{-1} (full width at half-height ~500 cm^{-1}). This solution spectrum is shown in Figure 3, which also contains room-temperature solid-state (Nujol mull) spectra of $[N(n\text{-}Bu)_4^+][H(OTeF_5)_2^-]$, $[N(n\text{-}Bu)_4^+][D(OTeF_5)_2^-]$, and $N(n\text{-}Bu)_4Cl$. The broad band at 1150 cm^{-1} in the $H(OTeF_5)_2^-$ spectra is clearly shifted to lower energy in the $D(OTeF_5)_2^-$ spectrum. Less clearly seen is the 3% shift to lower energy upon deuterium substitution of a band assigned to $\nu(TeO)_{asym}$, from 766 to 741 cm^{-1}. Although we prepared $[N(n\text{-}Bu)_4^+][D(OTeF_5)_2^-]$ from $DOTeF_5$ that was 95% D, the maximum % D that we have achieved in the $D(OTeF_5)_2^-$ salt is ~80%. Both $DOTeF_5$ and $[N(n\text{-}Bu)_4^+][D(OTeF_5)_2^-]$ undergo H/D exchange upon aging, presumably by reacting with adventitious water. Thus, spectrum C in Figure 3 contains ~20% $[N(n\text{-}Bu)_4^+][H(OTeF_5)_2^-]$ (estimated by ^1H NMR spectroscopy). Spectra of samples containing 50:50 $H(OTeF_5)_2^-$:$D(OTeF_5)_2^-$ (not shown) clearly show both bands at 766 and 741 cm^{-1}. Furthermore, when the sample that produced spectrum C in Figure 3 was exposed to air, the spectrum changed to one identical with spectrum B in Figure 3 in less than 5 min. Adequate control experiments (^1H and ^{19}F NMR) demonstrated that no reaction other than H/D exchange occurred during this brief exposure to air. The bands assigned to $\nu(OH)_{asym}$ (1150 cm^{-1}) and $\nu(TeO)_{asym}$ (766 cm^{-1}) do not

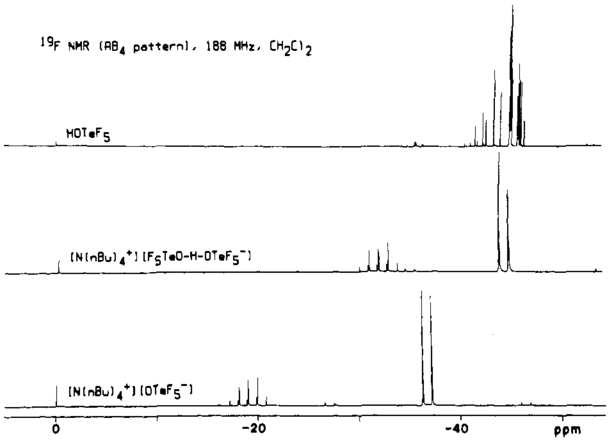

Figure 2. Fluorine-19 NMR spectra.

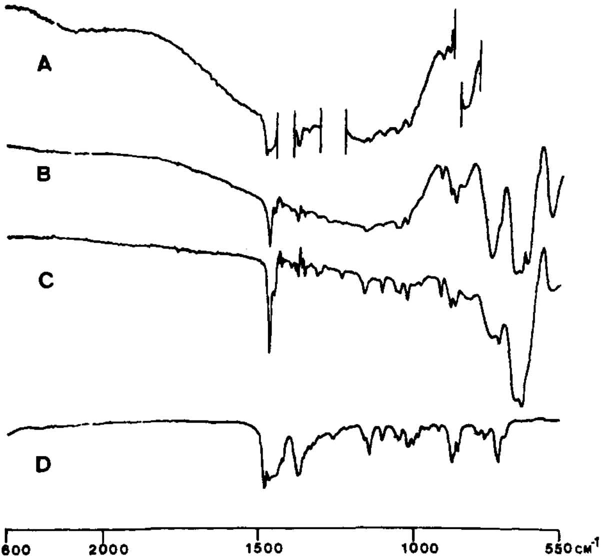

Figure 3. Infrared spectra (22 °C) of a dichloromethane solution of $[N(n\text{-}Bu)_4^+][H(OTeF_5)_2^-]$ (A) and Nujol mulls of $[N(n\text{-}Bu)_4^+][H(OTeF_5)_2^-]$ (B), $[N(n\text{-}Bu)_4^+][D(OTeF_5)_2^-]$ ca. 80% D (C), and $N(n\text{-}Bu)_4Cl$ (D).

---

(29) Schomaker, V.; Trueblood, K. N. *Acta Crystallogr., Sect. B: Struct. Crystallogr. Cryst. Chem.* **1968**, *B24*, 63.
(30) (a) Clark, J. H.; Emsley, J. *J. Chem. Soc., Dalton Trans.* **1974**, 1125. (b) Faithful, B. D.; Gillard, R. D.; Tuck, D. G.; Ugo, R. *J. Chem. Soc. A* **1966**, 1185.
(31) Fujiwara, F. Y.; Martin, J. S. *J. Am. Chem. Soc.* **1974**, *96*, 7625.
(32) (a) Poscham, W.; Engelbrecht, A. *Z. Phys. Chem. (Leipzig)* **1971**, *248*, 177. (b) Rode, B. M.; Engelbrecht, A.; Schantl., J. *Z. Phys. Chem. (Leipzig)* **1973**, *253*, 17.
(33) Seppelt, K. *Z. Anorg. Allg. Chem.* **1973**, *399*, 65.
(34) Engelbrecht, A.; Sladky, F. *Int. Rev. Sci.: Inorg. Chem. Ser. Two* **1975**, *3*, 137.

Table VI. IR and Raman Data (Stretching Frequencies, cm^{-1})[a]

compd	$\nu(OH)$[b] IR	$\nu(TeO)$ IR	$\nu(TeO)$ Raman	$\nu(TeF)$ IR	$\nu(TeF)$ Raman
$HOTeF_5$	3618 (22)[c] 3424 (177)[e]	733, 740 sh[c,d] *f*		733, 740[c,d] *f*	
$DOTeF_5$	2670 (15)[c] 2536 (100)[e]	734[c,d] *f*		734[c,d] *f*	
$[N(n\text{-}Bu)_4^+][OTeF_5^-]$		867 (18) 861 (10)[e]	866 (18)	636 (17) 641 (14)[e,g]	644 (6), 575 (6)
$[NEt_3H^+][OTeF_5^-]$		853 (52)	850 (10)	645 (66)	654 (7), 590 (8)
$[N(n\text{-}Bu)_4^+][H(OTeF_5)_2^-]$	1150 (400) 1150 (400)[e]	850 w, 766 s	848[h]	689, 674, 654	673 (9), 621 (8)
$[N(n\text{-}Bu)_4^+][D(OTeF_5)_2^-]$	700–800	741 s		689, 674, 654 sh	

[a] Solid-state spectra unless otherwise indicated. Values in parenthesis are bandwidths at half-height (cm^{-1}). sh = shoulder, bd = broad, w = weak, s = strong. [b] $\nu(OD)$ for deuterated compounds. [c] Gas phase. [d] Combination of $\nu(TeO)$ and $\nu(TeF)$. See ref 24. [e] Dichloromethane solution. [f] This region of the spectrum is below the cutoff of the solution cell with Irtran-2 windows (~775 cm^{-1}). [g] Solution cell with KBr windows used. [h] Only observed below 150 K.[35]

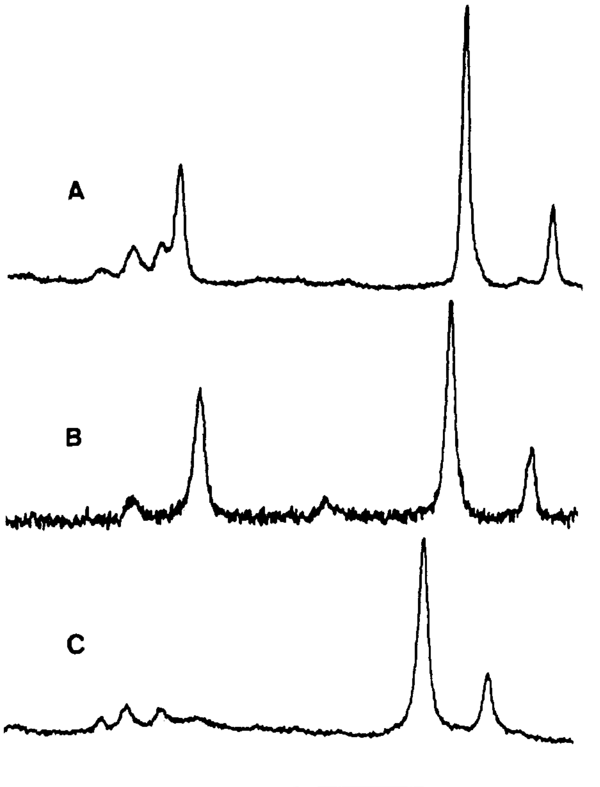

Figure 4. Raman spectra (22 °C) of powders of $[N(n\text{-}Bu)_4^+][OTeF_5^-]$ (A), $[NEt_3H^+][OTeF_5^+]$ (B), and $[N(n\text{-}Bu)_4^+][H(OTeF_5)_2^-]$ (C).

change in appearance or position at 140 K, the temperature of the X-ray diffraction study.[35]

Figure 4 displays Raman spectra of $[N(n\text{-}Bu)_4^+][OTeF_5^-]$, $[NEt_3H^+][OTeF_5^-]$, and $[N(n\text{-}Bu)_4^+][H(OTeF_5)_2^-]$. The prominent features in the 550–700-cm^{-1} region are two A_1 $\nu(TeF)$ bands, which are seen to shift to higher energy as the net negative charge on the teflate oxygen atom decreases.

Discussion

Comparison of $H(OTeF_5)_2^-$ to Other Teflate Compounds. A large number of compounds containing $OTeF_5$ groups have been prepared and characterized.[1-3] Studies that are relevant to this discussion include structural characterization by electron diffraction[36] and X-ray diffraction[8b,10,11,37,38] and spectroscopic investigations by vibrational[24,39-41] and ^{19}F NMR[33,34] spectroscopy.

Table VII. Spectroscopic and Structural Data for Representative $OTeF_5$ Compounds

compd	$\nu(TeO)$,[a] cm^{-1}	Te–O dist, Å	δ_A[b]
$B(OTeF_5)_3$	<740[c]	1.874 (6)[d]	−46.2[e]
$HOTeF_5$	734[f,g]		−42.4[g]
$[N(n\text{-}Bu)_4^+][B(OTeF_5)_4^-]$	795[e]		−38.3[e]
$[Au(OTeF_5)_3]_2$	812[h,i]	1.91 (2)[i]	
$Pt(OTeF_5)_2(NBD)$	816[j,k]		−33.2[j]
$[N(n\text{-}Bu)_4^+][H(OTeF_5)_2^-]$	808[g,l]	1.798 (4), 1.802 (4)[g]	−32.0[g]
$[AgOTeF_5(C_6H_5CH_3)_2]_2$	827[m,n]	1.789 (3)[n]	−29.9[n]
$Mn(CO)_5(OTeF_5)$	848[o]	1.75 (1)[o]	−30.8[o]
$[NEt_3H^+][OTeF_5^-]$	852[g]		−25.4[g]
$[N(n\text{-}Bu)_4^+][OTeF_5^-]$	867[g]		−19.0[g]

[a] Solid-state IR data unless otherwise noted. [b] ^{19}F NMR chemical shift (CH_2Cl_2, 22 °C, $CFCl_3$ internal standard) of fluorine trans to oxygen. [c] Highest energy band attributable to $\nu(TeO)$ or $\nu(TeF)$: Kropshofer, H.; Leitzke, O.; Peringer, P.; Sladky, F. *Z. Anorg. Allg. Chem.* **1973**, *399*, 65. [d] Reference 37d. [e] Strauss, S. H.; Abney, K. D., unpublished data. [f] Gas-phase spectrum; this single band is a combination of $\nu(TeO)$ and $\nu(TeF)$. See ref 24. [g] This work. [h] From Raman spectrum of the solid. [i] Reference 38. [j] Reference 12; NBD = norbornadiene. [k] Average of two observed IR bands, 805 and 827 cm^{-1}. [l] Average of two observed IR bands, 850 and 766 cm^{-1}. [m] Average of IR (819 cm^{-1}) and Raman (836 cm^{-1}) bands from spectra of the solid. [n] Reference 11. [o] Reference 10.

The extent of O-to-Te p–d π-bonding is very sensitive to the environment of the teflate oxygen atom. As the Te–O π-bonding decreases, the Te–O distance increases while the Te–O stretching frequency ($\nu(TeO)$) decreases and the chemical shift of the fluorine atom trans to oxygen (δ_A) shifts upfield. These correlations are clearly shown in Table VII. The free $OTeF_5^-$ anion has the maximum amount of O-to-Te π-bonding, resulting in the strongest (and presumably shortest[42]) Te–O bond with the highest $\nu(TeO)$. As the interaction of any other element with the teflate oxygen atom increases, O-to-Te π-bonding decreases, progressively weakening and lengthening the Te–O bond. An extreme example is seen in the compound $B(OTeF_5)_3$, with a Te–O distance of 1.874 (6) Å.[37d] In this case O-to-B p–p π-bonding severely limits the double-bond character of the Te–O bond. The benchmark for a Te–O single bond distance is 1.91 Å, the average of the Te–O distances found in the monoclinic modification of $Te(OH)_6$.[43]

The structural and spectroscopic parameters for $H(OTeF_5)_2^-$ (Table VII) show that this species contains teflate groups that

---

(35) Swanson, B. I.; Abney, K. D.; Strauss, S. H., unpublished data.
(36) Oberhammer, H.; Seppelt, K. *Inorg. Chem.* **1978**, *17*, 1435.
(37) (a) Pritzkow, H.; Seppelt, K. *Inorg. Chem.* **1977**, *16*, 2685. (b) Lentz, D.; Pritzkow, H.; Seppelt, K. *Ibid.* **1978**, *17*, 1926. (c) Huppmann, P.; Labischinski, H.; Lentz, D.; Pritzkow, H.; Seppelt, K. *Z. Anorg. Allg. Chem.* **1982**, *487*, 7. (d) Sawyer, J. F.; Schrobilgen, G. J. *Acta Crystallogr., Sect. B: Struct. Crystallogr. Cryst. Chem.* **1982**, *B38*, 1561.
(38) Huppmann, P.; Hartl, H.; Seppelt, K. *Z. Anorg. Allg. Chem.* **1984**, *524*, 26.
(39) Mayer, E.; Sladky, F. *Inorg. Chem.* **1975**, *14*, 589.
(40) Sladky, F.; Kropshofer, H.; Leitzke, O.; Peringer, P. *J. Inorg. Nucl. Chem., Suppl.* **1976**, 69.
(41) Schack, C. J.; Wilson, W. W.; Christe, K. O. *Inorg. Chem.* **1983**, *22*, 18.
(42) The Te–O distance in free $OTeF_5^-$ is not known, since salts such as $Cs^+OTeF_5^-$ are at least threefold disordered in the solid state.[40]
(43) Lindquist, O.; Lehman, M. C. *Acta Chem. Scand.* **1973**, *27*, 85.

are a compromise between the covalent and ionic extremes, represented by $HOTeF_5$ and $OTeF_5^-$, respectively. Figure 2 shows that δ_A for $H(OTeF_5)_2^-$ (−32.0) is close to the −30.7 average for $HOTeF_5$ and $OTeF_5^-$ (δ_A −42.4 and −19.0, respectively). It is clear that the spectrum labeled "$[F_5TeO\text{-}H\text{-}OTeF_5^-]$" in Figure 2 does not arise from a mixture of $HOTeF_5$ and $OTeF_5^-$ rapidly equilibrating via proton transfer, since the average δ_B for these two species is far from δ_B for $H(OTeF_5)_2^-$. Other spectroscopic data (^1H NMR and infrared), discussed below, demonstrate that the solid-state structure persists in solution and that the equilibrium in eq 1 lies far to the left. The ^{19}F NMR data for $H(OTeF_5)_2^-$ are in harmony with the Te–O distances, which are the same to within one standard deviation and average 1.800 (6) Å. This value is midway between the extremes expected for a Te–O single-bond distance, ~1.91 Å (see above), and for the Te–O bond distance in $OTeF_5^-$, which is probably ~1.70 Å.[42,44]

$$H(OTeF_5)_2^- \xrightleftharpoons{CH_2Cl_2} HOTeF_5 + OTeF_5^- \qquad (1)$$

With Table VII as a guide, the structural and ^{19}F NMR data suggest that $\nu(TeO)$ for $H(OTeF_5)_2^-$ would be found at ~820 cm^{-1}. The Te–O oscillators are vibrationally coupled in our compound, with $\nu(TeO)_{asym}$ and $\nu(TeO)_{sym}$ found at 766 (strong) and 850 (weak) cm^{-1}, respectively. The average of these values is 808 cm^{-1}, very close to the expected value. This coupling is not unexpected: the centrosymmetric dimer $[AgOTeF_5(C_6H_5CH_3)_2]_2$, which contains a planar Ag_2O_2 core, has $\nu(TeO)_{asym}$ = 819 cm^{-1} (IR active only) and $\nu(TeO)_{sym}$ = 836 cm^{-1} (Raman active only).[11] Since $H(OTeF_5)_2^-$ is not centrosymmetric, the symmetric stretch, although very weak, is infrared active and is observed below 150 K.[35] It is not clear why $\nu(TeO)_{sym}$ is only seen in the Raman spectrum below 150 K.[35] This matter is under further investigation.

Comparison of $H(OTeF_5)_2^-$ with Bifluoride (HF_2^-). Many reviews that discuss the bifluoride ion are available.[14-19] This anion contains the shortest, strongest hydrogen bond. In most cases, the proton is confined to a symmetrical, single minimum potential between the closely spaced fluoride ions (2.27 (1) Å, cation dependent[45]).[46] The hydrogen bond energy of bifluoride, i.e. the enthalpy change of eq 2, has recently been determined to be 39 (1) kcal/mol in an important ion cyclotron resonance study of ion–molecule clustering equilibria.[47] Such a determination cannot be made at present for $H(OTeF_5)_2^-$ because the masses involved are too large. We have heated the compound $[N(n\text{-}Bu)_4^+][H(OTeF_5)_2^-]$ to 40 °C under vacuum for 24 h without any liberation of $HOTeF_5$ (bp 60 °C[4]), suggesting that the enthalpy change for eq 3 is positive and large. Vibrational spectra of $[N(n\text{-}Bu)_4^+][H(OTeF_5)_2^-]$ in dichloromethane show no trace of $\nu(OH)$ for $HOTeF_5$ at 3424 cm^{-1}, demonstrating that the equilibrium in eq 1 lies far to the left. Furthermore, the ^1H NMR chemical shift of the bridging proton in $H(OTeF_5)_2^-$ is nearly invariant to changes in solvent (Table IV), suggesting that even the basic solvent acetonitrile does not compete with $OTeF_5^-$ for the proton donor $HOTeF_5$.

$$HF_2^-(g) \rightarrow HF(g) + F^-(g) \qquad (2)$$

$$[N(n\text{-}Bu)_4^+][H(OTeF_5)_2^-](s) \rightarrow HOTeF_5(g) + [N(n\text{-}Bu)_4^+][OTeF_5^-](s) \qquad (3)$$

Table VIII. Spectroscopic and Structural Data for HA_2^- Ions

acid HA	pK_a[a]	counterion	O···O in HA_2^-, Å	$\nu(OH)_{asym}$ in HA_2^-, cm^{-1}
CH_3COOH	13.0	Na^+	2.44 (1)[b]	720[c,d]
CCl_3COOH	12.2	Rb^+	2.455[e]	850[e]
CF_3COOH	11.4	K^+	2.437 (4)[f]	850[c,d]
HNO_3	10.1	Cs^+	2.468 (8)[g]	600[h]
$HOTeF_5$	8.8	$N(n\text{-}Bu)_4^+$	2.595 (8)[i] (2.564)	1150[i]
HSO_3F	6.1	Cs^+	2.41 (1)[j]	
C_6H_5COOH		K^+	2.51 (4)[k]	1200[c]
$p\text{-}ClC_6H_4COOH$		K^+	2.46 (1)[l]	1220[c]
$p\text{-}CH_3OC_6H_4COOH$		K^+	2.48 (2)[m]	1100[c]

[a] Measured in acetic acid at 25 °C. See ref 32. [b] Speakman, J. C.; Mills, H. H. *J. Chem. Soc.* **1961**, 1164. [c] Reference 54. [d] Hadzi, D.; Orel, B.; Novak, A. *Spectrochim. Acta, Part A* **1973**, *29A*, 1745. [e] Hadzi, D.; Obradovic, M.; Orel, B.; Solmajer, T. *J. Mol. Struct.* **1972**, *14*, 439. The O···O distance comes from the thesis of F. Lazarini, University of Ljubljana, 1972, and is cited in this reference without a standard deviation. [f] MacDonald, A. L.; Speakman, J. C.; Hadzi, D. *J. Chem. Soc., Perkin Trans. 2* **1972**, 825. [g] Roziere, J.; Roziere-Bories, M. T.; Williams, J. M. *Inorg. Chem.* **1976**, *15*, 2490. [h] Detoni, S.; Diop, L.; Gunde, R.; Hadzi, D.; Orel, B.; Potier, A.; Potier, J. *Spectrochim. Acta, Part A* **1979**, *35A*, 443. [i] This work. The value in parentheses is the O···O distance corrected for librational motion. [j] Belin, C.; Charbonnel, M.; Potier, J. *J. Chem. Soc., Chem. Commun.* **1981**, 1036. [k] Skinner, J. M.; Stewart, J. M.; Stewart, G. M. D.; Speakman, J. C. *J. Chem. Soc.* **1954**, 180. [l] Mills, H. H.; Speakman, J. C. *J. Chem. Soc.* **1963**, 4355. [m] McGregor, D. R.; Speakman, J. C. *J. Chem. Soc. A* **1968**, 2106.

Since the hydrogen bond enthalpy for $H(OTeF_5)_2^-$ cannot be measured directly, a convenient and straightforward alternative is to estimate the strength of the bond from the O···O distance. As the hydrogen bond between two species A–H and B becomes stronger, the A–H bond distance increases and the A···B distance decreases.[14-19] Thus, the strongest hydrogen bonds have the longest A–H and shortest A···B distances. Even after we account for the smaller radius of fluorine as compared with that of oxygen (the covalent[48] and van der Waals[28] radii being respectively 0.64 and 0.66 Å and 1.35 and 1.40 Å), the 2.595 (8) Å O···O distance in $H(OTeF_5)_2^-$ (2.564 Å with librational correction) suggests a much weaker hydrogen bond than in HF_2^-. In fact, the shortest distances between two oxygen atoms bridged by a proton are in the range 2.29–2.34 Å,[49-51] considerably shorter than the distance in our compound. We do not think that steric repulsions between teflate groups prevent the oxygen atoms from getting closer than ~2.6 Å. Our conclusion is based on the availability of two internal degrees of freedom by which the O1···O2 distance could be made shorter *without* causing shorter F···F distances. If one assumes that the bridging hydrogen atom lies on the O1···O2 vector, the Te1–O1–H and Te2–O2–H angles of 112.8 and 112.3° are significantly more acute than previously determined angles at teflate oxygen atoms, which range from 132 to 180°.[8b,10,11,37,38] If these angles or the dihedral angle between the Te1–O1–O2 and Te2–O2–O1 planes (113°) were more obtuse, any steric repulsions between the two teflate groups in the $H(OTeF_5)_2^-$ ion would decrease, allowing the O1···O2 distance to decrease as well. Note that the compound $F_5TeOOTeF_5$ probably has a O–O distance of <1.5 Å, since it has a relatively strong O–O bond.[52] The existence of this stable peroxide demonstrates that two $OTeF_5$ groups can easily be much closer together than observed in the $H(OTeF_5)_2^-$ ion.

Comparison of $H(OTeF_5)_2^-$ with Other O–H–O Hydrogen Bonds. The most interesting aspect of this work is the apparent paradox that arises when one compares the structure of $[N(n\text{-}Bu)_4^+][H(OTeF_5)_2^-]$ with spectroscopic data for this compound.

---

(44) From the data in Table VI, we feel it is reasonable to argue that the Te–O distance in $OTeF_5^-$ is probably less than 1.75 (1) Å, the value found for $Mn(CO)_5(OTeF_5)$.[10] Note that the Xe–O distance in $[(XeOF_4)_3F^-]$ is 1.70 (5) Å: Holloway, J. H.; Kaucic, V.; Martin-Rovet, D.; Russell, D. R.; Schrobilgen, G. J.; Selig, H. *Inorg. Chem.* **1985**, *24*, 678.

(45) (a) Peterson, S. W.; Levy, H. A. *J. Chem. Phys.* **1952**, *20*, 704. (b) McDonald, T. R. R. *Acta Crystallogr.* **1960**, *13*, 113. (c) McGaw, B. L.; Ibers, J. A. *J. Chem. Phys.* **1963**, *39*, 2977. (d) Ibers, J. A. *Ibid.* **1964**, *40*, 402.

(46) When the fluoride ions are in dissimilar crystallographic environments, the proton is closer to one fluoride; i.e., the potential is still a single minimum but is not symmetric: Williams, J. M.; Schneemeyer, L. F. *J. Am. Chem. Soc.* **1973**, *95*, 5780.

(47) Larson, J. W.; McMahon, T. B. *J. Am. Chem. Soc.* **1982**, *104*, 5848.

(48) Reference 28, p 224.

(49) Bertrand, J. A.; Black, T. B.; Eller, P. G.; Helm, F. T.; Mahmood, R. *Inorg. Chem.* **1976**, *15*, 2965.

(50) Abu-Dari, K.; Raymond, K. N.; Freyberg, D. P. *J. Am. Chem. Soc.* **1979**, *101*, 3688.

(51) Bino, A.; Cotton, F. A. *J. Am. Chem. Soc.* **1979**, *101*, 4150.

(52) Seppelt, K. *Z. Anorg. Allg. Chem.* **1973**, *399*, 87.

Table IX. Spectroscopic and Structural Data for Some O–H–O Hydrogen Bonds

compd	R(O···O), Å	R(O–H), Å	ν(OH), cm^{-1}
$[N(n\text{-}Bu)_4^+][H(OTeF_5)_2^-]$	2.595 (8)[a] (2.564)		1150[a]
KHC_2O_4	2.518 (3)[b]	1.054 (5)[b]	1500[c]
HCOOH	2.58[d]		2650[e]
$NaHCO_3$	2.59[f]		2540[g]
$KH_3(SeO_3)_2$	2.566 (1), 2.602 (2)[h]	1.044 (7), 1.029 (3)[h]	
$KHCO_3$	2.585 (2)[i]		2630[g]
H_2SeO_3	2.621 (2), 2.667 (2)[j]	1.009 (3), 0.986 (3)[j]	
CH_3COOH	2.631 (8)[k]	1.011 (15)[k]	2875[l]
H_2SO_4	2.63[m]		3030[n]

[a] This work. The value in parentheses is the O···O distance corrected for librational motion. [b] Moore, F. H.; Power, L. F. *Inorg. Nucl. Chem. Lett.* **1971**, *7*, 873. Einspahr, H.; Marsh, R. E.; Donohue, J. *Acta Crystallogr., Sect. B: Struct. Crystallogr. Cryst. Chem.* **1972**, *B28*, 2194. [c] De Villepin, J.; Novak, A. *Spectrosc. Lett.* **1971**, *4*, 1. [d] Holtzberg, F.; Post, B.; Fankuchen, I. *Acta Crystallogr.* **1953**, *6*, 127. [e] Millikan, R. C.; Pitzer, K. S. *J. Am. Chem. Soc.* **1958**, *80*, 3515. [f] Sass, R. L.; Scheuerman, R. F. *Acta Crystallogr.* **1962**, *15*, 77. [g] Novak, A.; Saumagne, P.; Bok, L. D. C. *J. Chim. Phys. Phys.-Chim. Biol.* **1963**, *60*, 1385. [h] Lehman, M. S.; Larsen, F. K. *Acta Chem. Scand.* **1971**, *25*, 3859. [i] Thomas, J. O.; Tellgren, R.; Olovsson, I. *Acta Crystallogr., Sect. B: Struct. Crystallogr. Cryst. Chem.* **1974**, *B30*, 1155. [j] Larsen, F. K.; Lehman, M. S.; Sotofte, I. *Acta Chem. Scand.* **1971**, *25*, 1233. [k] Jonsson, P. G. *Acta Crystallogr. Sect B: Struct. Crystallogr. Cryst. Chem.* **1971**, *B27*, 893. [l] Haurie, M.; Novak, A. *Spectrochim. Acta* **1965**, *21*, 1217. [m] Pascard-Billy, C. *Acta Crystallogr.* **1965**, *18*, 829. [n] Goypiron, A.; De Villepin, J.; Novak, A. *Spectrochim. Acta, Part A* **1975**, *31A*, 805.

The O1···O2 distance of 2.595 (8) Å (2.564 Å with librational correction) is characteristic of moderately strong hydrogen bonds while vibrational and ^{1}H NMR data are characteristic of strong or very strong hydrogen bonds, i.e. those with O···O distances <2.5 Å.[53-55] Table VIII contains a list of O···O distances and $\nu(OH)_{asym}$ for a number of acid salts containing discrete HA_2^- ions (A^- = the anion of a hydroxy-containing acid). Since the pK_a for many of the parent acids HA have been determined in acetic acid solvent,[32] these data are also included. There is no apparent trend in O···O distance as a function of acidity of HA; the most acidic (HSO_3F) and least acidic (CH_3COOH) produce HA_2^- ions that exhibit the shortest O···O distances. Characteristic of all HA_2^- species is a $\nu(OH)_{asym}$ band in the IR spectrum that is very broad and shifted to ≤1200 cm^{-1}.[53-55] A band at 1150 cm^{-1} is attributed to $\nu(OH)_{asym}$ in $H(OTeF_5)_2^-$: this band shifts to lower energy in $D(OTeF_5)_2^-$ (Figure 3). Since the shape and position of this band are the same in dichloromethane solution and in the solid state, we conclude that the solid-state structure of $H(OTeF_5)_2^-$ is maintained in solution. The data in Table VIII, representative of all HA_2^--containing acid salts,[53] show that the O···O distance in $H(OTeF_5)_2^-$ is nearly 0.1 Å longer than in other HA_2^- species. Therefore, since the 2.595 (8) Å O···O distance in our compound (2.564 Å with librational correction) is not the result of crystal-packing forces or, as discussed above, the result of intramolecular steric repulsions, we must conclude that this distance is governed by electronic forces. At present we cannot offer a compelling explanation for this observation.

All known O–H–O hydrogen bonds with O···O distances ~2.6 Å have one relatively short and strong O–H bond. The hydrogen atom is found in a potential well (frequently with a fairly symmetric double minimum) with one O–H distance <1.1 Å and one H···O distance >1.5 Å. Table IX lists some representative data. Despite the O1···O2 distance of 2.595 (8) Å (2.564 Å with librational correction), several lines of evidence support the tentative and interesting conclusion that the hydrogen atom in $H(OTeF_5)_2^-$ is much closer to the midpoint of the O1···O2 vector than is normal for the observed O1···O2 distance. The ^{1}H NMR chemical shift for the $H(OTeF_5)_2^-$ ion is far downfield, suggesting a strongly deshielded bridging hydrogen atom. The assignment of $\nu(OH)_{asym}$, if correct, suggests that even the stronger of the two O–H bonds in $H(OTeF_5)_2^-$ is fairly weak. More convincing, however, are the results that indicate that the two teflate groups in the $H(OTeF_5)_2^-$ ion are very similar structurally and spectroscopically. While a dynamic disorder of the type O–H···O ⇌ O···H–O would lead to two averaged $OTeF_5$ groups, the thermal parameters for the two oxygen atoms do not show any observable evidence of a disorder in Te–O distances. We would expect a difference in Te–O distances of >0.1 Å if the teflate groups in $H(OTeF_5)_2^-$ were in substantially different environments (Table IV). The oxygen atom thermal ellipsoids would be elongated along the Te–O vectors if two such Te–O distances were averaged. Instead, the shortest axis of the oxygen atom thermal ellipsoids lies along the Te–O vectors. Finally, if the teflate groups were substantially different, two sets of ν(TeF) bands would be expected in the Raman spectrum of $[N(n\text{-}Bu)_4^+][H(OTeF_5)_2^-]$, one pair of A_1 stretching bands for each type of teflate group. In contrast, one pair of *slightly broadened* bands is observed (Figure 4, Table VI), suggesting a near equivalence of the $OTeF_5$ groups. Interestingly, at 15 K the 673-cm^{-1} Raman band is resolved into two peaks separated by 5 cm^{-1}.[35] This phenomenon will be carefully studied in an ongoing investigation.[35]

In summary, while there is no precedent for an O–H–O hydrogen bond to have an O–H distance >1.1 Å *and* and O···O distance >2.5 Å,[56] such a situation in $[N(n\text{-}Bu)_4^+][H(OTeF_5)_2^-]$ is supported by several lines of evidence. Further experiments are planned for this interesting compound, including neutron diffraction, variable-temperature (room temperature to <10 K) infrared and Raman spectroscopy, and incoherent inelastic neutron scattering.

Acknowledgment is made to the Research Corp., to the donors of the Petroleum Research Fund, administered by the American Chemical Society, and to the National Science Foundation (Grant CHE-8419719) for the support of this research. We thank Professors J. R. Norton and A. T. Tu for the use of their IR and Raman spectrometers, respectively, Dr. B. I. Swanson and S. Ekberg for recording the low-temperature IR and Raman spectra, and P. K. Miller, J. H. Reibenspies, C. K. Schauer, R. E. Miller, and M. M. Miller for experimental assistance. The Nicolet R3m/E diffractometer and computing system was purchased with funds provided by the National Science Foundation (Grant CHE-8103011).

Note Added in Proof. We have prepared $H^{18}OTeF_5$, $[N(n\text{-}Bu)_4^+][^{18}OTeF_5^-]$, and $[N(n\text{-}Bu)_4^+][H(^{18}OTeF_5)_2^-]$ (Miller, P. K.; Strauss, S. H., manuscript in preparation). The IR spectrum of the latter compound confirms our assignments of $\nu(TeO)_{sym}$ and $\nu(TeO)_{asym}$, which shift from 850 and 766 cm^{-1}, respectively, for the natural-abundance compound to 814 and 730 cm^{-1}, respectively, for the oxygen-18 compound.

Registry No. $HOTeF_5$, 57458-27-2; $[N(n\text{-}Bu)_4^+][OTeF_5^-]$, 102648-79-3; $[N(n\text{-}Bu)_4^+][H(OTeF_5)_2^-]$, 102648-80-6; $Te(OH)_6$, 11120-48-2; HSO_3F, 7789-21-1; $[N(n\text{-}Bu)_4^+][SO_3F^-]$, 88504-81-8; $[N(n\text{-}Bu)_4^+][H(SO_3F)_2^-]$, 102648-82-8; $[NEt_3H^+][OTeF_5^-]$, 102631-87-8; NEt_3, 121-44-8; D_2, 7782-39-0.

Supplementary Material Available: Listings of anisotropic thermal parameters for all non-hydrogen atoms (Table S-I) and hydrogen atom positions and isotropic thermal parameters (Table S-II), a drawing of the cation (Figure S-1), and a stereoview of the packing in the unit cell (Figure S-2) (4 pages). Ordering information is given on any current masthead page.

---

(53) Speakman, J. C. *Struct. Bonding (Berlin)* **1972**, *12*, 141.
(54) Hadzi, D.; Orel, B. *J. Mol. Struct.* **1973**, *18*, 227.
(55) Hadzi, D.; Bratos, S. In ref 17; Vol. 2, p 565.
(56) Olovsson, I.; Jönsson, P.-G. In ref 17; Vol. 2, p 393.